AIP | Applied Physics Letters

Erbium concentration control and optimization in erbium yttrium chloride silicate single crystal nanowires as a high gain material

Leijun Yin, David Shelhammer, Gejian Zhao, Zhicheng Liu, and C. Z. Ning

Citation: Applied Physics Letters **103**, 121902 (2013); doi: 10.1063/1.4821448
View online: http://dx.doi.org/10.1063/1.4821448
View Table of Contents: http://scitation.aip.org/content/aip/journal/apl/103/12?ver=pdfcov
Published by the AIP Publishing

Erbium concentration control and optimization in erbium yttrium chloride silicate single crystal nanowires as a high gain material

Leijun Yin, David Shelhammer, Gejian Zhao, Zhicheng Liu, and C. Z. Ning[a)]
ASU Nanophotonics Laboratory, Arizona State University, Tempe, Arizona 85287, USA

(Received 28 June 2013; accepted 1 September 2013; published online 16 September 2013)

Increasing erbium concentration while minimizing the reduction of photoluminescence is an important task for achieving erbium-based high-gain materials for integrated photonics applications. Here, we demonstrate a strategy of controlled variation of Erbium density in the growth of erbium yttrium chloride silicate (EYCS) ($(Er_xY_{1-x})_3(SiO_4)_2Cl$) single crystal nanowires by systematically varying x between 0 and 1. We show that, as a trade-off between high Er density and suppressed upconversion, Er composition $x = 0.3$ provides the best compromise with the strongest photoluminescence. This optimized Er-composition corresponds to an Er density of $5\times10^{21}\,cm^{-3}$, five times larger than the optimized Er density demonstrated previously for other thin film materials. We estimate that this optimized EYCS is promising in achieving optical gain exceeding 100 dB/cm.
 [http://dx.doi.org/10.1063/1.4821448]

One of the important tasks in integrated silicon photonics is to develop a high gain material which can be used to make compact amplifiers and coherent light sources. Erbium-containing materials are the ideal candidates due to the 1.5 μm emission from Er^{3+} ions. Unfortunately, Er density in a solid host is limited to only $10^{20}\,cm^{-3}$ due to clustering and segregation effects.[1] Such a low Er density leads to a small optical gain of only a few dB/cm, too small to be useful in compact devices. To increase the Er density, erbium compound materials with Er density over $10^{22}\,cm^{-3}$ were studied extensively.[2–7] It has been demonstrated that all or majority of Er ions in crystalline Er-compound materials are optically active,[4] unlike in Er-doped materials where only a small fraction of Er-ions are optically active. While realization of net optical gain still remains challenging in erbium compounds, such as erbium silicate,[2] erbium disilicate,[3] and erbium oxide,[5] a new compound named single crystal erbium chloride silicate (ECS),[6–8] synthesized in nanowire form, appears promising. The nanowire form enables higher crystal quality as compared to thin film.[9] Moreover, the nanowire itself provides a perfect cylindrical waveguide or cavity structure for the optical amplifiers or lasers.[10] Recently, 644 dB/cm signal enhancement has been demonstrated on a single ECS wire.[8] The estimated net gain is 76 dB/cm; however, such gain is much lower than the predicted optical gain which can be over a few hundreds of dB/cm. It indicates that only a limited amount of population inversion was achieved in ECS, very likely due to the cooperative upconversion (CU) effect. It is known that the CU effect becomes the main detrimental process when Er density is high since the Er-Er ion interaction increases with decreasing Er-Er distance.[11] In order to further increase optical gain, the Er density has to be controlled and optimized in single crystal compounds such as ECS. By decreasing the Er density in ECS to an optimized level, it should be possible to achieve higher net optical gain due to the reduced cooperative upconversion and thus increased population inversion.

Replacement of Er^{3+} ions with other rare earth ions of similar size is an effective way to control Er density. Yttrium (Y) is an ideal candidate, since Y ion (Y^{3+}) has an ionic radius of 90 pm, very close to that of the erbium ion (89 pm). By replacing Er^{3+} with Y^{3+}, Er-Y compounds with controllable Er densities have been demonstrated, e.g., $Er_xY_{2-x}O_3$,[12] $Er_xY_{2-x}SiO_5$,[13–15] and $Er_xY_{2-x}Si_2O_7$.[16] Although Er density can be varied continuously from $10^{20}\,cm^{-3}$ to $10^{22}\,cm^{-3}$ in these compounds, net optical gain has only been achieved when Er density is below $1.7\times10^{20}\,cm^{-3}$,[15] mainly because the upconversion process becomes less important and the lifetime becomes long enough only at such low Er density. Compared to Er-doped materials, Er compounds at such low Er density do not show particular advantage in producing high optical gain. In this work, we report on the synthesis and characterization of single crystal erbium yttrium chloride silicate (EYCS, $(Er_xY_{1-x})_3(SiO_4)_2Cl$) nanowires in which mole fraction x varies from 0 (yttrium chloride silicate, YCS) to 1 (ECS). The optimized Er density in EYCS is $5\times10^{21}\,cm^{-3}$ ($x = 0.3$), which shows the best trade-off between high Er density and suppressed upconversion. Such an optimized EYCS is promising in achieving optical gain over 100 dB/cm.

EYCS nanowires were grown using an Au-assisted chemical vapor deposition (CVD) method using the Vapor-Liquid-Solid growth mechanism, similar to the growth of ECS nanowires.[3,6] In a typical growth procedure, 50 mg of Si powder was loaded at the center of the tube furnace. Under a flow of 12 sccm Ar-5% H_2 gas, the tube furnace was pumped down to 3 Torr and heated up to 1150 °C. Anhydrous $ErCl_3$ and YCl_3 sources were mixed together in a 1 cm long quartz boat and loaded downstream at a position with temperature around 1070 °C. A Si wafer pre-sputtered with 12 nm of Au was used as the growth substrate and placed 0.5 cm away from the quartz boat. The growth temperature at the substrate location is estimated to be ~1040 °C. After 3 h of growth, the furnace was naturally cooled down to room temperature. By varying the amounts of $ErCl_3$ and YCl_3 sources, EYCS nanowires with

a)Author to whom correspondence should be addressed. Electronic mail: cning@asu.edu

different Er compositions (densities) were grown. The mole fractions of Er atoms in the source boat ($N_{Er}/(N_{Er}+N_Y)$) were 0, 0.02, 0.04, 0.11, 0.3, 0.53, 0.74, and 1. Photoluminescence (PL) measurements were performed under 665 nm, continuous-wave (CW) laser excitation at a photon flux of $2.5\times10^{20}\,cm^{-2}s^{-1}$. The PL signal was focused to the entrance slit of a 0.3 m long monochromator and detected by a LN_2 cooled InGaAs array detector. Time-resolved PL was measured using the same excitation laser but operated at pulse mode. The details of lifetime measurement can be found in Ref. 7. All the measurements were performed at room temperature.

Figure 1 shows the typical scanning electron microscopy (SEM) image and energy dispersive X-ray spectroscopy (EDX) spectrum of EYCS samples. The as-grown EYCS samples consist of dense nanowires with diameters ranging from tens of nanometers to over 1 μm, and lengths of around 20 μm. Although core-shell structure nanowires were reported on silicate nanowires using similar growth method,[3,6] we expect these nanowires are of the uniform composition without Si core due to the high growth temperature.[7] The EDX spectrum shows that the nanowires consist of five different elements: Er, Y, Si, O, and Cl. For EYCS samples grown with different amount of $ErCl_3$, the intensities of Si, O, and Cl signal peaks remain constant over all samples, while the Er signal decreases with decreasing mole fraction of Er in the source materials during growth. It indicates that Er density in the nanowires is related to the amount of $ErCl_3$ source. Quantitative analysis is shown in Fig. 3.

To study the crystal structures of these nanowires, X-ray diffraction (XRD) measurements were performed and the results are shown in Fig. 2. All samples show the same XRD pattern despite the intensity of some peaks fluctuating among different samples, due to the random orientation of the nanowires. The XRD patterns match well with the orthorhombic structure of ECS (PDF # 00-42-3065) and YCS (PDF #00-032-1430). The strongest peak corresponds to the diffraction pattern of the {060} plane. Overall, the EDX and the XRD patterns demonstrate that EYCS alloys with controllable Er density were synthesized. All measurements indicate that the crystal quality remains largely the same in the entire range of composition from pure ECS to pure YCS.

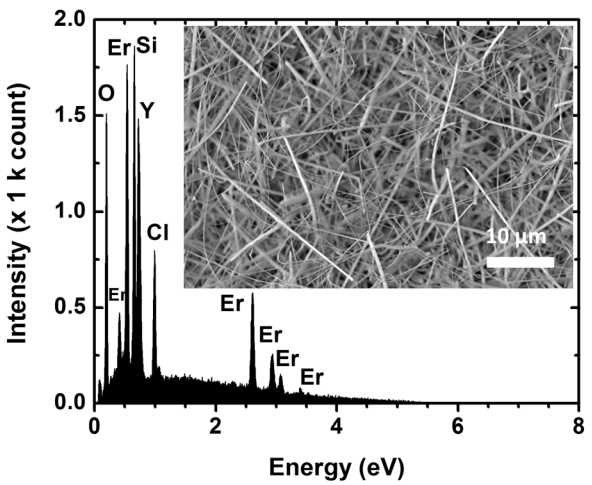

FIG. 1. The typical SEM image and EDX spectrum of EYCS nanowires.

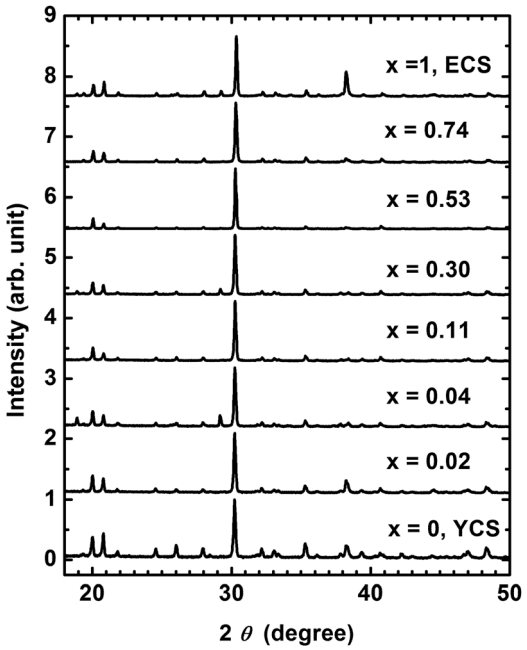

FIG. 2. XRD of $E_xY_{1-x}CS$ samples of different x values.

To determine the Er concentrations in different EYCS samples, three independent methods were used. In addition to XRD and SEM-EDX as described above, Rutherford back scattering (RBS) measurement was also carried out. In Fig. 2, it is clearly shown that EYCS samples synthesized from different amount of $ErCl_3$ and YCl_3 show similar XRD features. The small difference in size between Er^{3+} and Y^{3+} ions could result in a small change of the lattice constant. Fig. 3(a) shows the normalized high-resolution XRD measurements around 30 degrees in θ-2θ scans. While the higher peaks correspond to the {060} plane, the side peaks are attributed to the {230} plane. Clearly, the peak position shifts to larger angles when the atomic percentage of Er in the supplied source increases. This is consistent with decreasing {060} interplanar distance since Er^{3+} has a smaller crystal ionic radius than Y^{3+}. According to Bragg diffraction theory, the lattice spacing can be determined via the following equation:

$$\lambda = 2d_{EYCS}\sin\theta, \tag{1}$$

where $\lambda = 0.15418$ nm is the wavelength of Cu K_α line. The mole fraction of Er in EYCS, x, can be further obtained by linear interpolation of the {060} lattice spacing between pure ECS and pure YCS

$$d_{EYCS} = xd_{ECS} + (1-x)d_{YCS}, \tag{2}$$

where $d_{ECS} = 0.2942$ nm and $d_{YCS} = 0.2954$ nm. Based on the HR XRD result in Fig. 3(a), the atomic percentage of Er in EYCS is calculated as a function of mole fraction of Er in the supplied source during growth. The result is shown in Fig. 3(b). The Er atomic percentages measured from SEM-EDX and RBS are also plotted in this figure. Along the black line, the Er percentage in the product equals that in the supplied source. We notice that the Er atomic percentage measured by all three methods increases approximately linearly

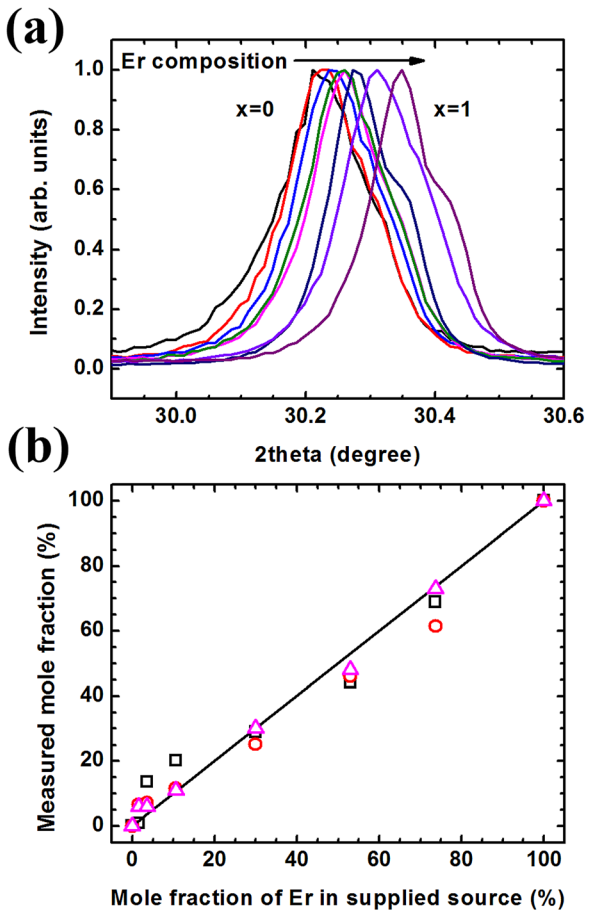

FIG. 3. (a) High resolution XRD spectra of EYCS samples, showing the peak shifting with the increasing Er composition from x = 0 to x = 1. (b) Measured x value of EYCS as a function of x value in the supplied sources by XRD (squares), EDX (open dots), and RBS (triangles). The black line illustrates the x value in the supplied source.

with the atomic percentage of Er in the supplied source. Among all three methods, RBS is known as the most accurate, and indeed, we found that the RBS result is the closest to the black line. We also notice that the x value determined by XRD deviates significantly from the black line when x is smaller than 0.2. This is due to the repeatability of the XRD measurement, around 0.01° for the employed instrument. Although the resolution of HR XRD measurements can be much better than 0.01°, the uncertainty of the absolute peak angle is limited by this repeatability. The 0.01° uncertainty in the angle does not affect the calculated atomic percentage much at high concentrations but causes significant deviation at low concentrations. Overall, the actual Er concentration in the EYCS nanowires matches well with the value in the growth sources. This result demonstrates direct control of Er density in EYCS using a CVD growth method.

The normalized high-resolution PL spectra at 1.5 μm of EYCS samples grown with different amounts of $ErCl_3$ source are shown in Fig. 4. The 1.5 μm emission is due to the radiative transition from the $^4I_{13/2}$ to the $^4I_{15/2}$ state of Er^{3+} ions. The nanowires grown with pure YCl_3 sources ($x = 0$, YCS) did not show any PL emission in this wavelength range because Y^{3+} ions do not have 4f electron transitions. All other samples grown with $ErCl_3$ sources exhibit a PL spectrum identical to that of ECS, indicating that Er ions in

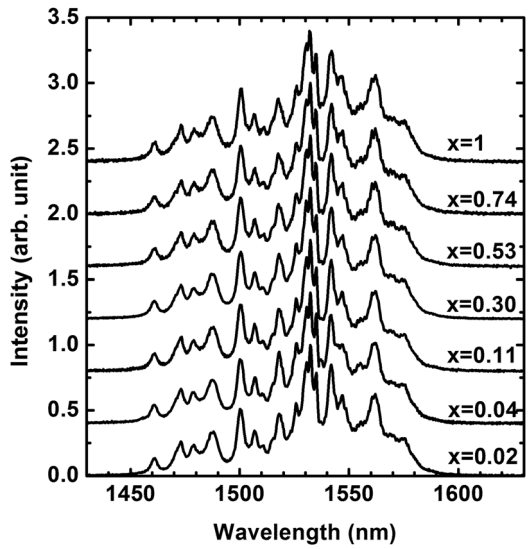

FIG. 4. Normalized PL spectra of $E_xY_{1-x}CS$ samples with different x values.

different samples are in the same crystal structure as ECS. The PL result again demonstrates that the synthesized nanowires samples are EYCS with different Er concentrations.

The PL lifetimes of the 1.53 μm emission of EYCS samples are measured in the same way as for ECS. Since the Er concentration has already been determined for different EYCS samples, the lifetime is plotted as a function of Er concentration for EYCS. As shown in Fig. 5(a), the lifetime increases from 410 μs for ECS to 3.7 ms for EYCS with x = 0.07, which corresponds to an Er density of 1.1×10^{21} cm^{-3}. Further decreasing the Er concentration might make the lifetime longer; however, the Er density is already in the same range as that achievable by traditional Er-doped materials. EYCS of such low Er density will not be of great interest. In order to find the best Er concentration, PL at the 1.5 μm band was measured for different as-grown EYCS samples under 665 nm laser excitation. Due to the spatial variation of wire density and morphology of the samples, the measured PL intensity varies from spot to spot on the as-grown sample. Statistical analyses of multiple PL measurements on each sample were carried out. The average integrated PL intensity of each sample together with its error bar is shown in Fig. 5(b). PL intensity reaches a maximum at $x = 0.3$ (corresponding to a volume density of 5×10^{21} cm^{-3}). In Ref. 7, we have shown that the lifetime density product (LDP) is a good measure of the PL intensity for different Er materials. The trade-off between lifetime and density results in an optimum Er density where the LDP is maximized. To compare the LDP and the integrated PL intensity, they were plotted in the same figure as a function of Er mole fraction. The LDP follows the same trend of increase as the integrated PL intensity at low Er densities up to $x = 0.3$, where the integrated PL starts to deviate from the behavior of the LDP and to decrease with increasing Er-density. We notice that the LDP is a good measure of the PL only if CU is ignored. Thus the decrease of PL at x = 0.3 indicates that the CU becomes important at the corresponding Er density (5×10^{21} cm^{-3}). A somewhat equivalent way of looking at the same data is the ratio of PL intensity to the PL lifetime, which is plotted in

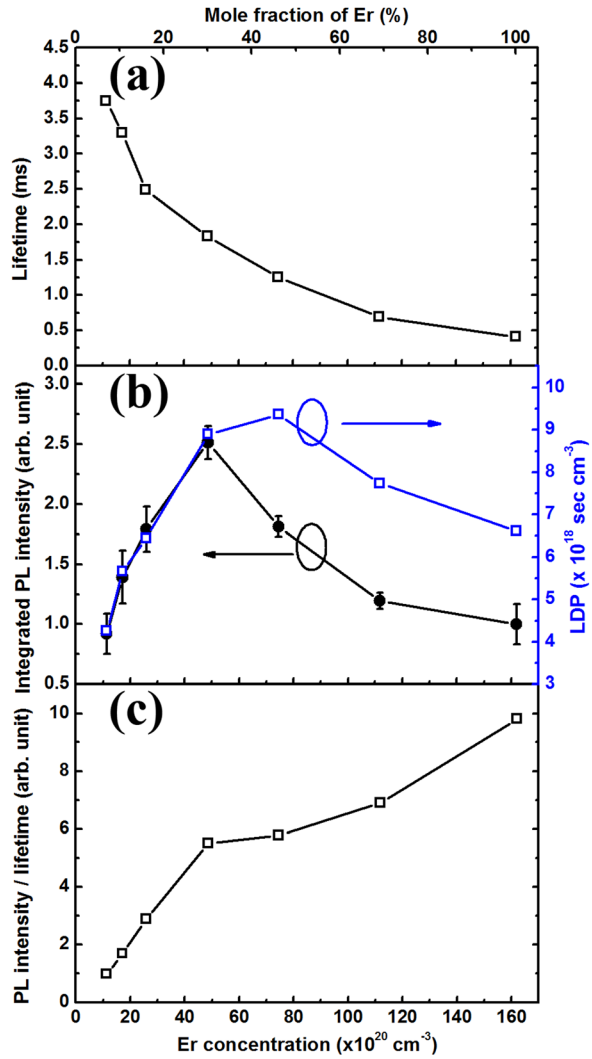

FIG. 5. (a) 1.5 μm PL lifetime of EYCS for different Er concentrations. (b) Comparison of integrated PL intensity at 1.5 μm and the lifetime density product at different Er concentrations. (c) PL intensity to lifetime ratio plotted against Er-concentration in EYCS.

Fig. 5(c) against total Er concentration. This ratio is usually used to determine the optically active percentage of Er ions out of the totally incorporated into a material.[1,17] As expected, this ratio increases first linearly with Er concentration up to $x = 0.3$, and increases sublinearly thereafter due to the CU processes which reduced both PL lifetime and intensity. We notice that this ratio serves poorly as a measure of active percentage of Er ions in compound crystal materials. But the initial linear regime does show similar behavior as in doped materials.

The alloy $Er_{0.3}Y_{0.7}CS$ represents the best trade-off between Er-density and CU, and thus the optimized Er-concentration. We notice that this optimized Er density in EYCS is about 5 times larger than the optimized density in $Er_xY_{2-x}SiO_5$ (Ref. 14) and $Er_xYb_{2-x}SiO_5$,[18] which is around $1\times10^{21}\,cm^{-3}$ ($x = 0.1$). The high optimized Er-density is due to the reduced CU effect in our EYCS nanowires as compared to other Er-compounds of the same Er density. The reduced upconversion is probably due to the smaller phonon energy in the EYCS crystal as a result of Cl atom being much heavier than O. Additionally, growth in nanowire form typically enables high crystal quality,[9] which leads to uniform Er distribution in the crystal and less quenching centers such as OH^- group.[19] Suh *et al*. found that the CU coefficient of $Er_xY_{2-x}SiO_5$ in nanocrystal form is 36 times smaller than that of the thin film,[13,15] demonstrating the advantage of Er nanomaterials. The EYCS nanowires take advantage of nanostructure properties and thereby demonstrate both higher Er density and suppressed upconversion simultaneously. The combination of high Er density ($5\times10^{21}\,cm^{-3}$), relative long lifetime (1.83 ms), and small CU makes this material very promising in achieving high optical gain. Since $Er_xY_{2-x}SiO_5$ reported in Ref. 13 is also in nanostructure form and have a high crystal quality, we assume the CU coefficient and absorption cross section of EYCS materials are similar. Theoretical calculation predicts its optical gain exceeding 100 dB/cm at a pump photon flux of $3\times10^{24}\,cm^{-2}s^{-1}$.

In summary, EYCS single crystal nanowires with controllable Er density were synthesized. The Er density can be controlled directly by varying the Er mole fraction in the supplied sources. The PL lifetime of EYCS decreases with increasing Er density as a result of concentration quenching. EYCS with $x = 0.3$ shows the strongest PL emission in the 1.5 μm band and insignificant CU. The optimized Er density in EYCS is five times higher than that achieved in other Er compounds such as $Er_xY_{2-x}SiO_5$ and $Er_xYb_{2-x}SiO_5$. Such an Er compound with high density, long lifetime, and small CU is potentially capable of achieving 100 dB/cm optical gain.

This work was initially carried out during a project supported by Army Research Office Award (W911NF-08-1-0471, Mike Gerhold) and has been mainly supported by AFOSR (FA9550-10-1-0444, Gernot Pomrenke). The authors would like to thank Dr. Barry Wilkens for the help of RBS measurement. We gratefully acknowledge the use of facilities within the LeRoy Eyring Center for Solid State Science at Arizona State University and specifically recognize D. Wright for his support on the glove box usage and for valuable discussions.

[1]A. Polman, J. Appl. Phys. **82**, 1 (1997).
[2]H. Isshiki, M. J. A. Dood, A. Polman, and T. Kimura, Appl. Phys. Lett. **85**, 4343–4345 (2004).
[3]H. J. Choi, J. H. Shin, K. Suh, H. K. Seong, H. C. Han, and J. C. Lee, Nano. Lett. **5**, 2432–2437 (2005).
[4]M. Miritello, R. L. Savio, F. Iacona, G. Franzò, A. Irrera, A. M. Piro, C. Bongiorno, and F. Priolo, Adv. Mater. **19**, 1582 (2007).
[5]S. Saini, K. Chen, X. Duan, J. Michel, L. C. Kimerling, and M. Lipson, J. Electron. Mater. **33**, 809–814 (2004).
[6]A. Pan, L. Yin, Z. Liu, M. Sun, P. L. Nichols, R. Liu, Y. Wang, and C. Z. Ning, Opt. Mater. Express **1**, 1202 (2011).
[7]L. Yin, H. Ning, S. Turkdogan, Z. Liu, P. L. Nichols, and C. Z. Ning, Appl. Phys. Lett. **100**, 241905 (2012).
[8]Z. C. Liu, L. J. Yin, and C. Z. Ning, in *CLEO, San Jose* (2013), CF1I.6.
[9]A. Pan, W. Zhou, E. S. P. Leong, R. Liu, A. H. Chin, B. Zou, and C. Z. Ning, Nano Lett. **9**, 784–788 (2009).
[10]M. Huang, S. Mao, H. Feick, H. Yan, Y. Wu, H. Kind, E. Weber, R. Russo, and P. Yang, Science **292**, 1897 (2001).
[11]P. G. Kik and A. Polman, J. Appl. Phys. **93**, 5008–5012 (2003).
[12]R. Lo Savio, M. Miritello, P. Cardile, and F. Priolo, J. Appl. Phys. **106**, 043512 (2009).
[13]K. Suh, J. H. Shin, S.-J. Seo, and B.-S. Bae, Appl. Phys. Lett. **92**, 121910 (2008).

[14]X. J. Wang, G. Yuan, H. Isshiki, T. Kimura, and Z. Zhou, J. Appl. Phys. **108**, 013506 (2010).
[15]K. Suh, M. Lee, J. S. Chang, H. Lee, N. Park, G. Y. Sung, and J. H. Shin, Opt. Express **18**, 7724–7731 (2010).
[16]M. Miritello, R. Lo Savio, P. Cardile, and F. Priolo, Phys. Rev. B **81**, 041411(R) (2010).
[17]A. Polman, G. N. van den Hoven, J. S. Custer, J. H. Shin, R. Serna, and P. F. A. Alkemade, J. Appl. Phys. **77**, 1256–1262 (1995).
[18]X. J. Wang, B. Wang, L. Wang, R. M. Guo, H. Isshiki, T. Kimura, and Z. Zhou, Appl. Phys. Lett. **98**, 071903 (2011).
[19]E. Snoeks, P. G. Kik, and A. Polman, Opt. Mater. **5**, 159–167 (1996).